JACS
JOURNAL OF THE AMERICAN CHEMICAL SOCIETY
ARTICLE
pubs.acs.org/JACS

Silylium−Arene Adducts: An Experimental and Theoretical Study

Muhammad Farooq Ibad,[†,‡] Peter Langer,[‡,§] Axel Schulz,[*,†,§] and Alexander Villinger[*,†]

[†]Abteilung Anorganische Chemie and [‡]Abteilung Organische Chemie, Institut für Chemie, Universität Rostock,
Albert-Einstein-Strasse 3a, D-18059 Rostock, Germany

[§]Leibniz-Institut für Katalyse e.V. an der Universität Rostock, Albert-Einstein-Strasse 29a, D-18059 Rostock, Germany

Supporting Information

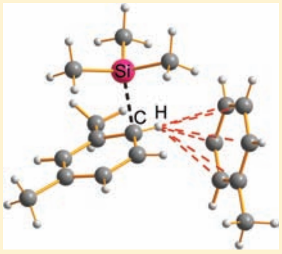

ABSTRACT: The solvent-coordinated [$Me_3Si\cdot$arene][$B(C_6F_5)_4$] salts (arene = benzene, toluene, ethylbenzene, *n*-propylbenzene, isopropylbenzene, *o*-xylene, *m*-xylene, *p*-xylene, 1,2,3-trimethylbenzene, 1,2,4-trimethylbenzene, 1,3,5-trimethylbenzene) are prepared and fully characterized. As an interesting decomposition product the formation of bissilylated fluoronium ion [$Me_3Si{-}F{-}SiMe_3$]$^+$ was observed and even cocrystallized with [$Me_3Si\cdot$arene][$B(C_6F_5)_4$] (arene = benzene and toluene). Investigation of the degradation of [$Me_3Si\cdot$arene][$B(C_6F_5)_4$] reveals the formation of fluoronium salt [$Me_3Si{-}F{-}SiMe_3$][$B(C_6F_5)_4$], $B(C_6F_5)_3$, and a reactive "C_6F_4" species which could be trapped with CS_2. Upon addition of CS_2, the formation of a formal *S*-heterocyclic carbene adduct, $C_6F_4CS_2{-}B(C_6F_5)_3$, was observed. The structure and bonding of substituted [$Me_3Si\cdot$arene][$B(C_6F_5)_4$] with arene = $R_nC_6H_{6-n}$ (R = H, Me, Et, Pr, and Bu; $n = 0{-}6$) is discussed on the basis of experimental and theoretical data. X-ray data of [$Me_3Si\cdot$arene][$B(C_6F_5)_4$] salts reveal nonplanar arene species with significant cation···anion interactions. As shown by different theoretical approaches (charge transfer, partial charges, trimethylsilyl affinity values) stabilizing inductive effects occur; however, the magnitude of such effects differs depending on the degree of substitution and the substitution pattern.

1. INTRODUCTION

Cations containing a tricoordinate silicon atom, R_3Si^+ (where R is an alkyl or aryl group), are known as silylium (also silylenium or silicenium) ions.[1,2] A long debate concerning the existence of "naked" R_3Si^+ cations (Chart 1, species A),[3] free of interactions with counterions (Chart 1, species B) and neighboring groups or solvent (Chart 1, species C and D), was finally brought to an end with the isolation and full characterization of [$(Mes)_3Si$][$HCB_{11}Me_5Br_6$]$\cdot C_6H_6$ (Mes = 2,4,6-trimethylphenyl) by the groups of Lambert and Reed in 2002.[4] The silylium ion in [$(Mes)_3Si$][$HCB_{11}Me_5Br_6$] was shown to be three-coordinate, planar, and well-separated from the carborane anions and benzene solvate molecules by means of single-crystal X-ray studies. *o*-Methyl groups of the bulky mesityl substituents shield the silicon atom from the close approach of nucleophiles, while remaining innocent as electron donors themselves.[4]

Silylium ions with their electron sextet and empty p orbitals are electron-deficient species and thus strong Lewis acids. Even relatively weak Lewis bases, such as π/σ donor solvents (e.g., toluene,[5] CH_3CN,[6] etc.), form tetrahedral complexes with silylium ions.[5] In addition, intramolecular π coordination in silylium ions containing a 2,6-diarylphenyl scaffold which adopt the C_1-symmetric geometry of a Wheland-like complex was observed (Chart 2, species E).[7] The first well-documented examples of intramolecular π-stabilization in silyl cations are silanorbornyl cations.[8]

As silylium ions are highly reactive Lewis acids, they are useful reagents in chemical synthesis.[9−15] Ozerov et al.[11] and Müller et al.[12] have utilized silylium ions as reactive catalysts for the activation of C−F bonds. The Ozerov group introduced a class of carborane-supported, highly electrophilic silylium compounds that act as long-lived catalysts for hydrodefluorination of trifluoromethyl and nonafluorobutyl groups by widely accessible silanes under mild conditions. The reactions are completely selective for aliphatic carbon−fluorine bonds in preference to aromatic carbon−fluorine bonds.[11b] Recently, Oestreich et al.[13] demonstrated that a tamed, ferrocene-based silylium ion (Chart 2, species F) catalyzes demanding Diels−Alder reactions in an unprecedented temperature range.

Both the utilization of chemically robust weakly coordinating anions[17,18] and the steric shielding of the Lewis-acidic Si atom[7,16] led to the structural determination of a silylium ion.[4] The first structurally characterized salt bearing a silylium cation, [Et_3Si]$^+$[$B(C_6F_5)_4$]$^-\cdot$2(toluene), was reported by Lambert et al. in 1993.[5] The crystal structure of [Et_3Si]$^+$[$B(C_6F_5)_4$]$^-\cdot$toluene revealed a silyl cation with significant coordination to a toluene molecule, which is the solvent for crystallization. The nature and extent of this coordination were controversial.[19,20] For a free R_3Si^+ cation, all three substituents should lie in a plane, and the average bond angle to the tricoordinate silicon should be 120°. However, for the Et_3Si^+ ion, the average angle was only 114°, and thus, [Et_3Si]$^+$[$B(C_6F_5)_4$]$^-\cdot$toluene should be regarded as a salt containing a solvent complex as a cation of the type [$Et_3Si\cdot$toluene]$^+$ (Chart 1, species C).

In contrast to the solid state, the free silylium cation in solution seems to be an exception (e.g., Mes_3Si^+)[21] due to interaction with the solvent.[22] The question is how much silylium cation character (if any at all) can be retained in a solvent-coordinated silylium

Received: October 18, 2011
Published: November 15, 2011

dx.doi.org/10.1021/ja209693a | J. Am. Chem. Soc. 2011, 133, 21016–21027

Chart 1. Silylium Ions[a]

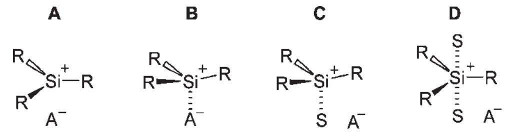

[a] Species description: A, naked cation; B, ion pair with strong cation−anion interactions; C and D, solvent complexes as cation (A^- = weakly coordinating anion, S = σ or π donor solvent).

Chart 2. Species E Showing Intramolecular π Coordination in Silylium Ions (R_1, R_2 = H, Me) and Species F, a Ferrocene-Based Silylium Ion Intramolecularly Stabilized by Electron-Rich Fe

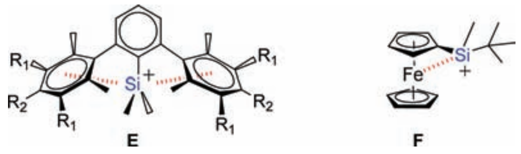

cation.[23] There is computational evidence that even argon can be a ligand to Me_3Si^+.[3a]

Ever since the isolation of $[Et_3Si\cdot toluene]^+$, no further solvent complex bearing a silylium solvent complex as a cation of the type $[R_3Si\cdot arene]^+$ (R = alkyl) has been isolated and structurally characterized. Recently, salts containing $[Me_3Si{-}X{-}SiMe_3]^+$ ions (X = halogen, pseudo-halogen), which can also be considered as solvent complexes of $Me_3Si{-}X$ and $[Me_3Si]^+$, have been described.[24] In these complexes the Me_3Si fragment has also almost completely lost its silylium character (strong deviation from planarity), since a stable covalently bonded tetracoordinated Si center is formed (Chart 1, species **C** with S = $Me_3Si{-}X$).[12,17b,24b,25]

Besides salts bearing $[R_3Si\cdot arene]^+$ or $[Me_3Si{-}X{-}SiMe_3]^+$ ions (X = halogen), a frequently used reagent in silylation chemistry is $[Et_3Si^+][B(C_6F_5)_4]$, first reported by Lambert.[5b,26] Only recently, Reed and Nava proved that the commonly used triethylsilyl or trimethylsilyl perfluorotetraphenylborate salts, $[R_3Si^+][B(C_6F_5)_4]$, were misidentified.[27] All known alkyl-substituted, formal "$[R_3Si^+][B(C_6F_5)_4]$" salts, prepared from $R_3Si{-}H$ and $[Ph_3C][B(C_6F_5)_4]$, form $[B(C_6F_5)_4]$ salts containing a hydride-bridged silane adduct cation of the type $[R_3Si{-}H{-}SiR_3]^+$.

Since the silylium ion became a focus of attention especially in catalysis,[9,11−13,15] and there is still a lack of data with respect to silylium solvent complexes, we have studied in detail the structure, bonding, and interaction of the Me_3Si^+ ion with differently substituted arenes of the type $R_nC_6H_{6-n}$, (R = H, Me, Et, Pr, and Bu; n = 0−6). By changing the substitution pattern and the size of the substituents (from small to bulky), we are able to discuss the steric and electronic influence on the solvent complex formation, which is, in addition, supported by computational data. Furthermore, we show that disproportionation may occur upon solvent complex formation when electron-rich *t*-Bu substituents are used.

2. RESULTS AND DISCUSSION

2.1. Synthesis of $[Me_3Si\cdot arene][B(C_6F_5)_4]$ Salts. As the Me_3Si^+ source, $[Me_3Si{-}H{-}SiMe_3][B(C_6F_5)_4]$ was always used and was reacted with a large excess of arene solvent. These Me_3Si^+ transfer reactions can be considered as Lewis acid−Lewis base reactions (see below). The solvent-coordinated $[Me_3Si\cdot arene][B(C_6F_5)_4]$ salts (arene = benzene, toluene, ethylbenzene, *n*-propylbenzene, isopropylbenzene, *o*-xylene, *m*-xylene, *p*-xylene, 1,2,3-trimethylbenzene, 1,2,4-trimethylbenzene, 1,3,5-trimethylbenzene, Figures 1−7) are easily obtained in 70−90% yields by treatment of neat $[Me_3Si{-}H{-}SiMe_3][B(C_6F_5)_4]$ with the corresponding arene solvent at ambient temperatures (Scheme 1). Gently heating to 80 °C affords a clear colorless solution with an oiled out layer. Slow cooling to ambient temperatures over a period of 1 h results in the deposition of colorless

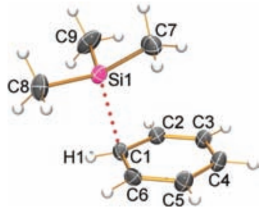

Figure 1. ORTEP drawing of the molecular structure of $[Me_3Si\cdot benzene]^+$. Thermal ellipsoids with 30% probability at 173 K.

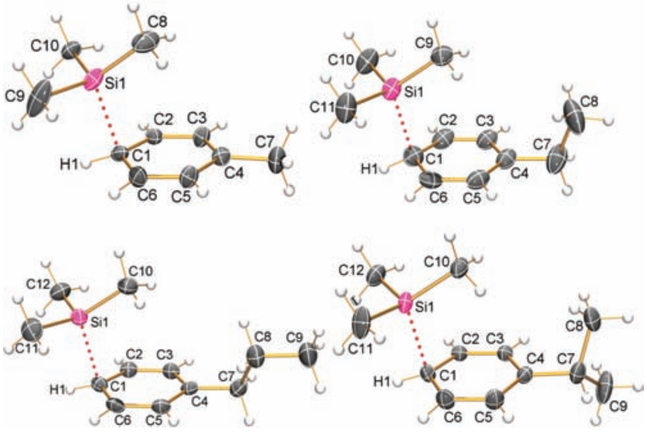

Figure 2. ORTEP drawing of the molecular structure of $[Me_3Si\cdot monosubstituted\_arene]^+$ (arene = toluene, ethylbenzene, *n*-propylbenzene, and isopropylbenzene). Thermal ellipsoids with 30% probability at 173 K.

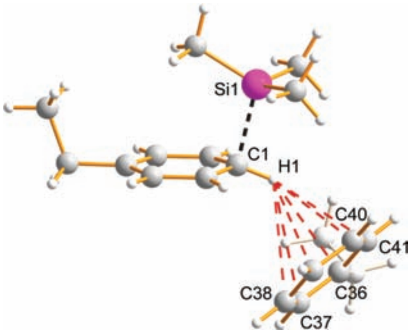

Figure 3. Short H1···C_{arene} distances (Å) (C36, 3.009; C37, 3.199; C38, 3.207; C39, 3.030; C40, 2.827; C41, 2.801) in the ethylbenzene adduct indicating weak van der Waals interactions in η^6 fashion with one solvent molecule.

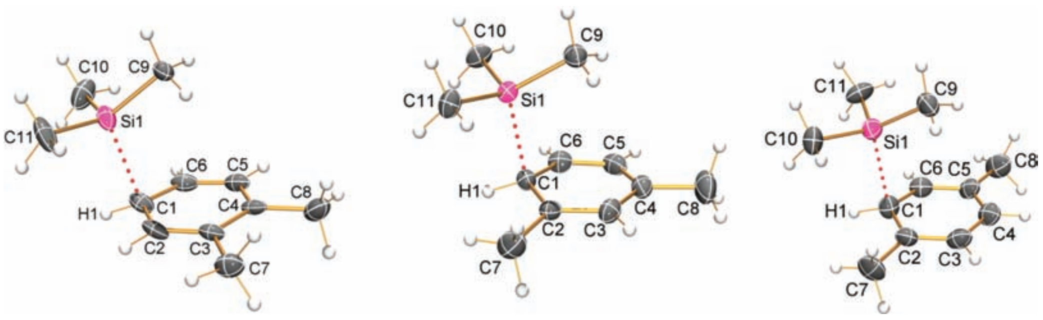

Figure 4. ORTEP drawing of the molecular structure of $[Me_3Si\cdot disubstituted\_arene]^+$ (arene = 1,2-dimethylbenzene, 1,3-dimethylbenzene, and 1,4-dimethylbenzene). Thermal ellipsoids with 30% probability at 173 K.

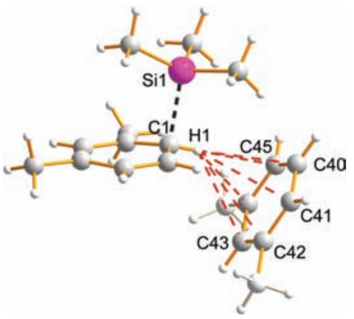

Figure 5. Short $H1\cdots C_{arene,solvent}$ distances (Å) (C37, 3.176; C38, 3.115; C39, 2.953; C40, 2.885; C41, 2.963; C42, 3.127) in the *m*-xylene adduct indicating weak van der Waals interactions in η^6 fashion with one solvent molecule.

crystals. Removal of excess arene by decantation and drying in vacuo gives the corresponding $[Me_3Si\cdot arene][B(C_6F_5)_4]$ salt with the solvent complex as the cation. It should be noted that it is difficult to obtain crystals suitable for a single-crystal X-ray analysis due to the low solubility of $[Me_3Si\cdot arene][B(C_6F_5)_4]$ salts in the corresponding solvents. To avoid thermal decomposition, the mixtures were carefully warmed with stirring until two clear colorless layers were obtained. Slow cooling to ambient temperature resulted in the deposition of large crystals rather than needlelike crystals or a crystalline slurry.

$[Me_3Si\cdot arene][B(C_6F_5)_4]$ salts are air and moisture sensitive but stable under an argon atmosphere over a long period as a solid but slowly decompose in solution even at ambient temperatures. Colorless crystals and solutions of $[Me_3Si\cdot arene][B(C_6F_5)_4]$ salts quickly turn yellow if traces of moisture are present. All $[Me_3Si\cdot arene][B(C_6F_5)_4]$ salts can be prepared in bulk and are almost indefinitely stable when stored in a sealed tube. They are thermally stable to over 80 °C. Between 88 °C (benzene) and 118 °C (1,2,3-trimethylbenzene, hemimellitene), decomposition occurs, which is presumably triggered by the formation of $Me_3Si{-}F$.

As an interesting side product, the formation of bissilylated fluoronium ion[25] $[Me_3Si{-}F{-}SiMe_3]^+$ was observed a few times and was even cocrystallized with $[Me_3Si\cdot arene][B(C_6F_5)_4]$ (arene = benzene, toluene) depending on the crystallization conditions (concentration, temperature, and time). Obviously, especially the weakest bound solvent complexes with benzene and toluene (see section 2.4) are reactive enough to slowly degrade the $[B(C_6F_5)_4]^-$ anion (Scheme 2) on gentle heating. A similar degradation of the $[B(C_6F_5)_4]^-$ ion has been reported before by Müller in naphthyl-based silylium ions.[12] We assume that the degradation proceeds via abstraction of a F^- ion by the reactive Me_3Si^+ ion, leading finally to the formation of the fluoronium salt $[Me_3Si{-}F{-}SiMe_3][B(C_6F_5)_4]$, $B(C_6F_5)_3$ and a reactive "C_6F_4" species. This assumption is supported by a trapping reaction with CS_2 as illustrated in Scheme 2. Upon addition of CS_2, the formation of a formal *S*-heterocyclic carbene (SHC) adduct, $SHC{-}B(C_6F_5)_3$, was observed besides $[Me_3Si{-}F{-}SiMe_3][B(C_6F_5)_4]$ and $B(C_6F_5)_3$. By fractional crystallization $SHC{-}B(C_6F_5)_3$ could be isolated in small quantities and characterized by single-crystal X-ray analysis. To the best of our knowledge 1,3-dithiol-2-ylidenes (Chart 3, structure A), which can be regarded as SHCs, are unknown since they immediately dimerize to well-known tetrathiafulvalenes (structure B).[28] The $SHC{-}B(C_6F_5)_3$ species is the first example of an *S*-heterocyclic carbene adduct complex with a Lewis acid.[29] Only recently Bertrand et al. reported on metal complexes (structure E) of the hitherto unknown 1,3-dithiol-5-ylidenes (structure D), which are isomers of SHC (structure A).[30]

All $[Me_3Si\cdot arene][B(C_6F_5)_4]$ salts have been fully characterized by elemental analysis, Raman and IR spectroscopy, and single-crystal structure elucidation.

2.2. Disproportionation Catalyzed by Silylium Ions: Friedel–Crafts Catalysis.

While the synthetic protocol described above worked nicely for benzene, toluene, ethylbenzene, *n*-propylbenzene, isopropylbenzene, *o*-xylene, *m*-xylene, *p*-xylene, 1,2,3-trimethylbenzene, 1,2,4-trimethylbenzene, and 1,3,5-trimethylbenzene, the same route yielded in the case of *tert*-butylbenzene two major products, $[Me_3Si{-}F{-}SiMe_3][B(C_6F_5)_4]$, which crystallizes first, and after concentration of the supernatant solution 1,4-di-*tert*-butylbenzene. Both products were identified by X-ray structure determination. This finding led to a detailed study of this disproportionation reaction which can be referred to as a Friedel–Crafts-type isomerization.[31] In the course of more than 120 years of Friedel–Crafts chemistry, two catalysts achieved preeminence: (i) anhydrous aluminum trichloride, which was introduced by Friedel and Crafts themselves, and (ii) boron trifluoride or the more convenient etherate–BF_3 complexes.[32] Since the 1960s, some superacid catalysts such as antimony pentafluoride gained significance.[33] Furthermore, the catalytic activity of superacids and metal triflate was intensively explored by Olah et al.[34] Also, Friedel–Crafts alkylations were already observed in C–F bond activation chemistry, e.g., as shown by the groups of Müller and Siegel.[35] Now, we can show that $[Me_3Si\cdot arene][B(C_6F_5)_4]$ salts are convenient and effective new Friedel–Crafts catalysts, which catalyze in the case of *tert*-butylbenzene the disproportionation, affording 1,3-di-*tert*-butylbenzene (8.47%), 1,4-di-*tert*-butylbenzene (64.4%), and 1,3,5-tri-*tert*-butylbenzene

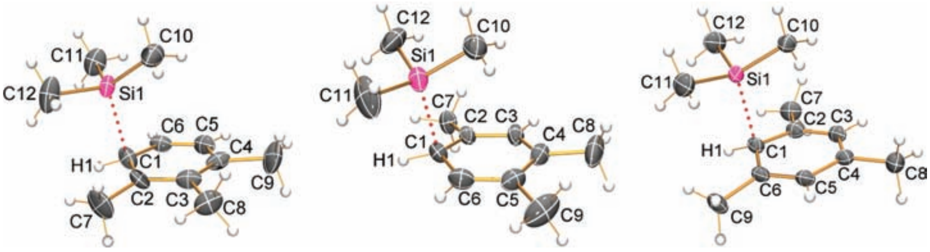

Figure 6. ORTEP drawing of the molecular structure of $[Me_3Si \cdot trisubstituted\_arene]^+$ (arene = 1,2,3-trimethylbenzene, 1,2,4-trimethylbenzene, and 1,3,5-trimethylbenzene). Thermal ellipsoids with 30% probability at 173 K.

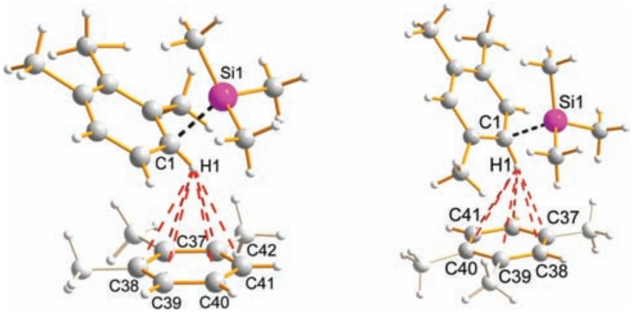

Figure 7. Short $H1 \cdots C_{arene,solvent}$ distances in 1,2,3-trimethylbenzene (Å) (C37, 2.999; C38, 3.141; C39, 3.216; C40, 3.013; C41, 3.154; C42, 3.013) and 1,2,4-trimethylbenzene adduct (Å) (C37, 2.898; C38, 2.898; C39, 3.067; C40, 3.228; C41, 3.228; C42, 3.067) indicating weak van der Waals interactions in η^6 fashion with one solvent molecule.

Scheme 1. Synthesis of $[Me_3Si \cdot arene][B(C_6F_5)_4]$ Salts

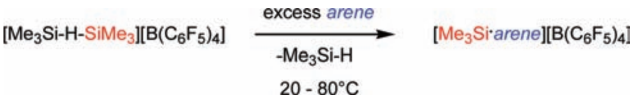

(27.2%) besides benzene as determined by GC/MS. The overall isolated yield is about 5.3% (referring to *tert*-butylbenzene) after 3 h at ambient temperatures or about 560% (referring to $[Me_3Si-H-SiMe_3][B(C_6F_5)_4]$). This corresponds to a turnover number (TON) of about 7.0 (referring to $[Me_3Si-H-SiMe_3][B(C_6F_5)_4]$, 3 h of reaction time). The long-term stability was also studied. Even after three days the catalyst was still active. Interestingly, also at −80 °C disproportionation was observed. The observation of predominant formation of the 1,4-di-*tert*-butylbenzene (64.4%) isomer can be explained only by intermolecular isomerization according to Scheme 3. Computations indicated that the silylium ion preferentially attacks at the *para* position (see section 2.4).

Disproportionation was only observed for the electon-rich *tert*-butylbenzene as the free *tert*-butyl species is more stable than other alkyl cations corresponding to the other substituted benzenes. For instance, in the case of *n*-propylbenzene and isopropylbenzene, no disproportionation was observed even after refluxing for several days at high temperatures in a sealed tube (T = 160 °C).

2.3. X-ray Crystallography. The structures of $[Me_3Si \cdot arene][B(C_6F_5)_4]$ salts (arene = benzene, toluene, ethylbenzene, *n*-propylbenzene, isopropylbenzene, *o*-xylene, *m*-xylene, *p*-xylene, 1,2,3-trimethylbenzene, 1,2,4-trimethylbenzene, 1,3,5-trimethylbenzene) and the decomposition products $[Me_3Si-F-SiMe_3][B(C_6F_5)_4]$ and $SHC-B(C_6F_5)_3$ have been determined. Tables S1−S6 in the Supporting Information present the X-ray crystallographic data. Selected molecular parameters are listed in Table 1. X-ray-quality crystals of all considered species were selected in Fomblin YR-1800 (Alfa Aesar) at ambient temperature. All samples were cooled to 173 K during the measurement.

2.3.1. $[\mathbf{Me_3Si \cdot benzene}][\mathbf{B(C_6F_5)_4}]$ crystallizes solvent free from benzene in the monoclinic space group $P2/c$ with four formula units per unit cell. Interestingly, slightly different cell and structural parameters are found for crystals from different experiments (structures A and B, Table 1; Tables S1, S7, and S8, Supporting Information). Depending on the crystallization conditions (time and temperature), the degradation product $[Me_3Si-F-SiMe_3][B(C_6F_5)_4]$ cocrystallizes with $[Me_3Si \cdot benzene][B(C_6F_5)_4]$, forming mixed crystals of the type $0.76[Me_3Si \cdot benzene][B(C_6F_5)_4] \cdot 0.24[Me_3Si-F-SiMe_3][B(C_6F_5)_4]$. Here, the position of one $[Me_3Si-benzene]^+$ cation was found to be partially occupied by a $[Me_3Si-F-SiMe_3]^+$ ion. The occupancy of each part was refined freely (0.525(2)/0.475(2)). Partial substitution of $[Me_3Si \cdot benzene]^+$ by $[Me_3Si-F-SiMe_3]^+$ ions leads to a change in the space group to $P2_1/c$ and eight formula units in the unit cell.

Although in all three structures the cations are well-separated from the $[B(C_6F_5)_4]$ anions, there are numerous very weak $H_{methyl,cation} \cdots C-F_{anion}$ and $H_{arene,cation} \cdots C-F_{anion}$ interactions. For instance, 21 such contacts are found for structure A (Table 1), all between 2.4 and 3.0 Å (cf. $\Sigma r_{vdW}(H \cdots F) = 2.9$ Å).[36]

The silicon atom in the cations is tetracoordinated with bonding angles around the Si atoms between 341.7° and 343.1°, displaying a strong deviation from planarity (360.0°) as well as from the value for an ideal tetrahedral environment (328.4°). Such relatively large $\Sigma\angle(Si)$ values[37] were reported for complexes between silylium ions and solvent molecules (341.4(5)° and 342.6(5)° for $[Et_3Si \cdot toluene][B(C_6F_5)_4]$)[6] and anions (345.0(10)° and 349.0(9)° for $[Et_3Si][Br_6CB_{11}H_6]$)[38] and for the bissilylated halonium ions (345−348° for $[Me_3Si-X-SiMe_3][B(C_6F_5)_4]$, X = halogen).[24b] A second interesting aspect of the structure is the intriguingly large distance between silicon and the fourth coordination site, the solvent benzene (Figure 1). The coordination mode of this interaction is clearly η^1 rather than η^2 or η^6 (cf. $d(Si-C1) = 2.174(2)$ Å vs $d(Si-C2) = 2.758(2)$ Å, $d(Si-C3) = 3.558(2)$ Å, $d(Si-C4) = 3.884$ Å, $d(Si-C5) = 3.562$ Å, and $d(Si-C6) = 2.758$ Å). The three slightly different Si−C1 distances (structures A−C, Table 1) both illustrate the huge influence of the environment due to a very flat potential energy surface and manifest the error of structure elucidation. The observed value of 2.169(3)−2.183(4) Å is considerably larger than the sum of the C and Si covalent radii (1.91 Å;[39] cf. 2.18 Å in $[Et_3Si \cdot toluene][B(C_6F_5)_4]$)[5] but still much shorter than the

Scheme 2. Degradation Reaction of $[Me_3Si\cdot arene][B(C_6F_5)_4]$ and Trapping of C_6F_4 by SHC Adduct Formation upon Addition of CS_2

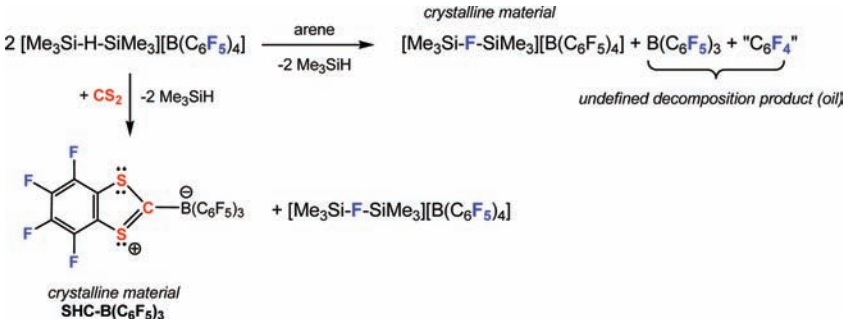

Chart 3. Structural Framework of Unknown SHCs = 1,3-Dithiol-2-ylidenes (A), Which Dimerize to Known Tetrathiafulvalenes (B), Adducts with Lewis Acids (C), and the Unknown 1,3-Dithiol-5-ylidene Isomer (D) and Its Known Adducts (E) (LA = Lewis Acid)

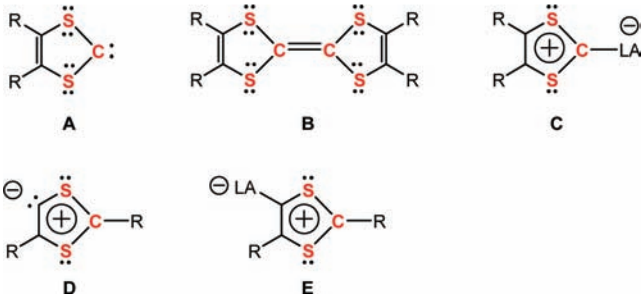

Scheme 3. Me_3Si^+-Catalyzed Isomerization Reaction Leading to the 1,4-Substituted Arene (R = *t*-Bu; Counterion = $[B(C_6F_5)_4]^-$)

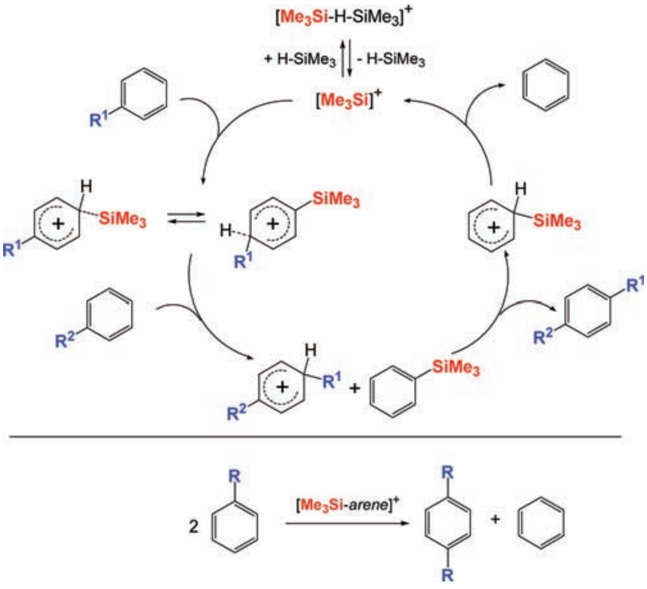

sum of the van der Waals radii (3.8 Å).[36] As a consequence of the Si···C1 interaction, the trigonal planar environment around C1 changes to strongly distorted tetrahedral, leading to an out-of-plane position for H1 as displayed by the H1−C1−C2−C6 dihedral angle (Table 1).

2.3.2. **$[Me_3Si\cdot RC_6H_5][B(C_6F_5)_4]$ (R = Me, Et, *n*-Pr, *i*-Pr)** crystallizes from RC_6H_5 in the orthorhombic space group *Pbca* (R = Me) or the monoclinic space groups $P2_1/n$ (Et) and $P2_1/c$ (*n*-Pr, *i*-Pr) with either four (R = Et, *i*-Pr) or eight (R = Me, *n*-Pr) formula units per unit cell. Again, for the toluene species it was possible to isolate mixed crystals of the type $0.92[Me_3Si\cdot toluene][B(C_6F_5)_4]\cdot 0.08[Me_3Si{-}F{-}SiMe_3][B(C_6F_5)_4]$ besides pure $[Me_3Si\cdot toluene][B(C_6F_5)_4]$. Both sorts of crystals have almost identical cell data.

In all four alkyl-substituted benzene adducts (Figure 2), the silylium cation attacks in the *para* position to the alkyl substituent and slightly shorter Si···C1 distances compared to those of the unsubstituted $[Me_3Si\cdot benzene]^+$ ion are observed in accord with the theoretical results (see section 2.1). In the case of the derivatives with longer alkyl side chains, the β C atom of the alkyl chain always adopts a *cis* position with respect to the silyl group. Similar to the $[Me_3Si\cdot benzene]^+$ ion, also all four alkyl-substituted benzene cations display very weak $H_{methyl,cation}\cdots C{-}F_{anion}$ and $H_{arene,cation}\cdots C{-}F_{anion}$ interactions. Among these four salts only the ethyl derivative crystallizes with one solvent molecule (EtC_6H_5) per cation. As can be seen from Figure 3, the solvent molecule is closely arranged to the cation and clearly directed toward the H1 proton in η^6-type coordination mode with $H_{arene,cation}\cdots C_{arene,solvent}$ distances between 2.80 and 3.20 Å (cf. Σr_{vdW} (H···C) = 3.1 Å).[36] This solvent···$H_{arene,cation}$ interaction is further supported by a significantly larger displacement of the H1 proton from the arene ring plane within the cation as indicated by the H1−C1−C2−C6 dihedral angle (−147.4° vs <−155° for all other species). Furthermore, natural population analysis (NPA) partial charge calculations reveal that H1 carries the largest positive charge (Table 2) with 0.32*e* (cf. 0.23*e*−0.27*e* for all other arene protons) and even the protons of the Me_3Si unit are less positive (0.27−0.29*e*). In the uncoordinated solvent the charges of all arene protons are all very similar and in the range of 0.23*e*−0.24*e*, displaying especially for H1 a large positive charge accumulation upon adduct formation. Comparison of the averaged $C_{arene}{-}C_{arene}$ distances in the ethylbenzene cation and the uncoordinated solvent molecule displays a shortening of these distances by ca. 0.025 Å. An even stronger effect is found for the $C_\beta{-}C_\gamma$ distance of the ethyl group, increasing by 0.049 Å in the cation, which might partly be attributed to a stronger hyperconjugative effect of the $C_\beta{-}C_\gamma$ σ bond with the π^* bond system of the arene upon attack of the silylium cation in the *para* position.

Table 1. Selected Structural Data of Experimentally Observed $[Me_3Si\cdot arene]^+$ Ions

arene		$d(Si1\cdots C1)$, Å	$\Sigma\angle(Si)$, deg	$\angle(H1-C1-C2-C6)$, deg
C_6H_6 (benzene)	A[a]	2.174(2)	341.7	−157.8
	B[a]	2.169(3)	341.8	−157.7
	C[b]	2.183(4)	343.1	−162.1
MeC_6H_5 (toluene)	A	2.135(5)	341.0	−156.0
	B[b]	2.120(2)	340.7	−158.9
EtC_6H_5		2.140(3)	341.5	−147.4
n-PrC_6H_5		2.137(2)	340.9	−159.4
i-PrC_6H_5		2.169(2)	342.1	−155.9
1,2-$Me_2C_6H_4$ (o-xylene)		2.137(3)	341.4	−158.0
1,3-$Me_2C_6H_4$ (m-xylene)		2.148(2)	338.3	−148.9
1,4-$Me_2C_6H_4$ (p-xylene)		2.167(5)	341.2	−155.6
1,2,3-$Me_3C_6H_3$		2.129(5)	339.2	−154.2
1,2,4-$Me_3C_6H_3$		2.121(3)	336.2	−155.2
1,3,5-$Me_3C_6H_3$		2.139(2)	334.2	−150.0
		2.171(6)[c]	336.5[c]	

[a] Two slightly different data sets. [b] Mixed crystals with $[Me_3Si-F-SiMe_3]^+$ ions. [c] Two independent molecules in the unit cell.

Table 2. Selected Structural Data of Experimentally Observed $[Me_3Si-F-SiMe_3]^+$ Ions

$[Me_3Si-F-SiMe_3][B(C_6F_5)]$	$d(Si-F)$, Å	$\angle(Si-F-Si)$, deg	$\Sigma\angle(Si)$, deg
$[Me_3Si\cdot C_6H_6][B(C_6F_5)]$[a]	1.708(7), 1.741(7)	159.0(6)	347.8, 347.9
$[Me_3Si\cdot MeC_6H_5][B(C_6F_5)]$[b]	1.73(2), 1.73(2)	158(2)	348.3, 348.0
pure salt[c]	1.753(9)	163.0(3)	348.0

[a] Cocrystallized bis(trimethylsilyl)fluoronium ion taken from structure C in Table 1. [b] Cocrystallized bis(trimethylsilyl)fluoronium ion taken from structure B in Table 1. [c] Taken from ref 25a.

2.3.3. $[Me_3Si\cdot Me_2C_6H_4][B(C_6F_5)_4]$. All three possible xylene derivatives (*ortho*, *meta*, and *para*) were synthesized (Figure 4). While *o*-xylene (1,2-dimethylbenzene) and *m*-xylene (1,3-dimethylbenzene) adducts crystallize in monoclinic space groups $P2_1/n$ and $P2_1/c$ with eight and four formula units, respectively, *p*-xylene (1,4-dimethylbenzene) crystallizes in the orthorhombic space group *Pbca* with eight molecules per unit cell. In the case of the *ortho* and *para* species, solvent molecules are included in the unit cell. However, only for the *ortho* species the η^6 coordination mode with the solvent—as described for $[Me_3Si\cdot EtC_6H_5][B(C_6F_5)_4]$ (Figure 3)—was observed, again with a stronger displacement of the H1 proton and fairly short $H1_{arene,cation}\cdots C_{arene,solvent}$ distances (Figure 5). For the *p*-xylene species, no such η^6 coordination arrangement was found and the shortest $H1\cdots C_{methyl}$ distance amounts to 3.592 Å, which was observed between H1 and one methyl carbon atom of the solvent molecule (cf. the shortest $H1_{arene,cation}\cdots C_{arene,solvent}$ distance, 4.417 Å). A comparison of the $Si\cdots C1$ distances with those of the benzene or monosubstituted species is not straightforward, since addition of the silyl group in the *para* position is not feasible in *p*-xylene. Thus, the most interesting question is the influence of the substitution pattern on the $Si\cdots C1$ distance within the group of xylene species. For the 1,2-substituted species, both (equivalent) *para* positions (C1/C6 in Figure 4) are energetically favored over all other possibilities. A similar situation is found for the 1,3-substituted cation, where the position at C1 (equivalent to C5) represents the *para* position (Figure 4). In the case of the 1,4-substituted species, adduct formation in the *para* position is rather unlikely due to steric repulsion with one methyl group in accord with theory (see section 2.4). Hence, only the *ortho* and *meta* positions are feasible (C1, C3, C5, and C6 are equivalent, Figure 4). As a result the longest $Si\cdots C1$ distance was found for *p*-xylene (2.167(5) Å, Table 1). The small difference between *o*- and *m*-xylene might be explained by the fact that in *o*-xylene the one *para* position and one *meta* position are energetically favored over one *para* position and one *ortho* position.

2.3.4. $[Me_3Si\cdot Me_3C_6H_3][B(C_6F_5)_4]$. Both the 1,2,3-trimethylbenzene (hemimellitene) adduct and the 1,2,4-trimethylbenzene (pseudocumene) adduct salts crystallize in the monoclinic space group $P2_1/c$ with four formula units, while the 1,2,4-trimethylbenzene (mesitylene) adduct salt crystallizes in $P\bar{1}$ with four formula units and two independent $[Me_3Si\cdot Me_3C_6H_3][B(C_6F_5)_4]$ species (Figure 6). Always one solvent molecule per $[Me_3Si\cdot Me_3C_6H_3][B(C_6F_5)_4]$ moiety is included in the unit cell of all three salts. For the 1,2,3- and the 1,2,4-trimethylbenzene adduct species, the solvent is again in the vicinity of the H1 proton as observed for $[Me_3Si\cdot EtC_6H_5][B(C_6F_5)_4]$ and the 1,2-substituted $[Me_3Si\cdot Me_2C_6H_4][B(C_6F_5)_4]$ (Figure 7). In the mesitylene species the solvent molecules are well separated from the cations, but as found for all other species weak $H_{methyl,cation}\cdots C-F_{anion}$ and $H_{arene,cation}\cdots C-F_{anion}$ interactions are also observed.

In the case of 1,2,3-trimethylbenzene, three *para* positions are available (C1 equivalent to C5, and C6). The silylium ion prefers for energetic reasons (see section 2.4) to attack position C1/C5 (one *para*, one *ortho*, and one *meta* C atom) rather than C6 with one *para* and two *meta* carbon atoms. For 1,2,3-trimethylbenzene there are three different adduct ions possible: (i) attached to C1 with one *para*, one *ortho*, and one *meta* position, (ii) attached

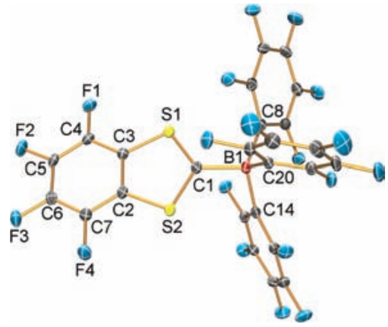

Figure 8. ORTEP drawing of the molecular structure of SHC−$B(C_6F_5)_3$ in the crystal. Thermal ellipsoids with 30% probability at 173 K. Selected bond lengths (Å) and angles (deg): S1−C1, 1.669(2); S1−C3, 1.728(2); S2−C1, 1.691(2); S2−C2, 1.735(2); C1−B1, 1.660(2); C2−C7, 1.390(3); C2−C3, 1.393(2); C3−C4, 1.394(2); C8−B1, 1.652(3); C14−B1, 1.654(3); C20−B1, 1.639(3); C1−S1−C3, 97.82(9); C1−S2−C2, 97.18(8); B1−C1−S1, 123.0(1); B1−C1−S2, 121.0(1); S1−C1−S2, 115.5(1); C7−C2−C3, 120.0(2); C7−C2−S2, 125.3(1); C3−C2−S2, 114.6(1); C2−C3−C4, 119.9(2); C2−C3−S1, 114.8(1); C4−C3−S1, 125.2(1); C3−S1−C1−B1, 173.5(1); C3−S1−C1−S2, 0.7(2); C2−S2−C1−B1, −174.0(1); C2−S2−C1−S1, −1.1(1); C1−S2−C2−C7, 179.0(2); C1−S2−C2−C3, 1.2(2).

to C3 with no *para* but two *ortho* positions and one *meta* position, and (iii) attached to C6 with one *ortho* and two *meta* positions. Since *para* position attack is preferred, the most stable isomer is the one where the silyl group attacks C1 in accord with theory (see below and the Supporting Information). For mesitylene only one isomer is possible since all three hydrogen-substituted arene carbon atoms are equivalent. Note: Adduct formation at an arene carbon atom attached to a methyl group is always unfavorable.

2.3.5. Molecular Structure of $[Me_3Si{-}F{-}SiMe_3]^+$ *Ions Co-crystallized in* $[Me_3Si\cdot benzene][B(C_6F_5)_4]$ *and* $[Me_3Si\cdot toluene][B(C_6F_5)_4]$. While the molecular structure of the pure salt is ideal C_2 symmetric, the symmetry is decreased to C_1 for the fluoronium cations in the mixed crystals (Table 2). Thus, slightly different Si−F bond distances are observed which range from 1.708(7) to 1.73(2) Å (cf. 1.753(9) Å for the pure salt). The largest difference is found for the Si−F−Si angles, which are somewhat smaller for the cations in the mixed crystals (158°/159° vs 163°), and this can be attributed to a very flat energy potential for the variation of the Si−F−Si angle.

2.3.6. **SHC-$B(C_6F_5)_3$** crystallizes in the monoclinic space group $P2_1/n$ with eight formula units per unit cell and two independent molecules. The planar SHC and the $B(C_6F_5)_3$ group (Figure 8) are connected by means of a strong B−C donor−acceptor bond that amounts to 1.660(2) Å (cf. Σr_{cov}(B−C) = 1.60 Å[39] and 1.641(2) Å in (1,3,4,5-tetramethylimidazol-2-ylidene)tris(pentafluorophenyl)borane[40] or 1.649(3) Å in the carbene adduct of 1,3-di-*tert*-butylimidazolin-2-ylidene with tris(pentafluorophenyl)borane),[41] which is slightly longer than those found for the $B{-}C_{C_6F_5}$ rings (d(C8−B1) = 1.652(3) Å, d(C14−B1) = 1.654(3) Å, d(C20−B1) = 1.639(3) Å).[42] The boron atom of $B(C_6F_5)_3$ is tetracoordinated, while the carbene carbon atom sits in an almost trigonal planar environment (∠(B1−C1−S1) = 123.0(1)°, ∠(B1−C1−S2) = 121.0(1)°, ∠(S1−C1−S2) = 115.5(1)°). The coordination geometry around boron in the BC_4 core is slightly distorted with the smallest angle 102.2(2)° and the largest 114.7(1)°. Two sets of different S−C bond distances are found: (i) Two rather short bond lengths of d(S1−C1) = 1.669(2) Å and d(S2−C1) = 1.691(2) Å are determined for the bonds to the carbene carbon atom, while (ii) slightly larger distances (d(S1−C3) = 1.728(2) Å and d(S2−C2) = 1.735(2) Å) are found for the two other $S{-}C_{ring}$ bonds. All four S−C bond lengths are considerably shorter than the sum of the covalent radii (Σr_{cov}(S−C) = 1.78 Å),[39] thus indicating partial double bond character within the five-membered C_3S_2 heterocycle.

2.4. Computations. Since very flat potential energy surfaces are observed for the systems $[Me_3Si\cdot arene]^+$ with respect to C−Si−C and Si−C1−H1 angles and the Si···C1 distance, consistent trends are only obtained for isolated species in the gas phase when environmental effects are excluded. All calculations were carried out with the Gaussian 03 package of molecular orbital programs.[43] The structures of silylium−arene adducts and the free arenes were optimized within the DFT approach at the pbe1pbe level with an aug-cc-pVDZ basis set.[44] Vibrational frequencies were also computed to include zero-point vibrational energies and thermal corrections in thermodynamic parameters and to characterize all structures as minima on the potential energy surface. A natural bond orbital (NBO) analysis[45] was performed at the same level to study the charge distribution, bond polarization, and hybridization effects.

2.4.1. Structure and Isomers. It is common knowledge that a tetracoordinated Si atom is tetrahedral and its tricoordinated species mostly trigonal planar.[1−17] However, the question arises as to the structure of a silylium derivative in which one coordination site is significantly more weakly bound, being in the range of a transition between a covalent bond and a van der Waals interaction. Of special interest is the effect of delocalization and substitution on the structure and energetics of the different possible isomers for the studied system $[Me_3Si\cdot arene]^+$. Selected experimental and computed structural data (of the lowest lying isomers) are given in Tables 1 and 3, respectively.

Comparison of our gas-phase geometry with the crystal structure shows a general agreement, within experimental errors. For instance, according to Table 1, the difference in the Si···C1 bond length scatters about 0.015 Å, the angle sum around Si about 1.4°, and the dihedral angle H1−C1−C2−C6 about 4.4°.

All considered $[Me_3Si\cdot arene]^+$ groups are nonplanar with Si···C1 distances between 2.196 Å ($[Me_3Si\cdot benzene]^+$) and 2.112 Å ($[Me_3Si\cdot 1,3,5\text{-}i\text{-}Pr_3C_6H_3]^+$). More sensitive with respect to the substitution pattern is the angle sum around Si (Σ∠(Si)) ranging between 342.4° ($[Me_3Si\cdot benzene]^+$) and 333.2° ($[Me_3Si\cdot 1,3,5\text{-}i\text{-}Pr_3C_6H_3]^+$). In the case of ($[Me_3Si\cdot C_6Me_6]^+$) an even smaller angle sum (Σ∠(Si)) of 331.2° is computed due to steric repulsion between the methyl group attached to the arene C1 atom and the three methyl groups of the Si atom. In all other species the silylium ion is always attached to a C1 atom bearing a hydrogen atom. Only very minor changes are observed for the C1−H1 distances, which only slightly increase upon substitution (1.095−1.099 Å).

In general, with increasing degree of substitution, the Si···C1 bond lengths decrease (C_6H_6, 2.196 Å; $Me_1C_6H_5$, 2.132 Å; $Me_2C_6H_4$, 2.132 Å;$Me_3C_6H_3$, 2.125 Å; $Me_4C_6H_2$, 2.123 Å; $Me_5C_6H_1$, 2.113 Å; Table 3), Σ∠(Si) decreases (cf. 342.4°, 341.0°, 338.5°, 335.0°, 334.5°, and 334.0°), while the C1−H1 bond lengths are almost not affected by the higher degree of substitution (cf. 1.0952, 1.0955, 1.0964, 1.0970, 1.0970, and 1.0971 Å). In Me_6C_6 the situation changes significantly since the C1 arene ring atom is now attached to a methyl group, introducing steric strain, which leads to a longer Si···C1 bond but a smaller value for Σ∠(Si).

Table 3. Theoretically Obtained Selected Structural Data (Distances, Å; Angles, deg) of Substituted $[Me_3Si\cdot arene]^+$ and $[Me_3Si-H-SiMe_3]^+$ Ions Along with Partial Charges (e) and the Overall Charge Transfer (e)

cation[d]	q_{Si}	Q_{CT}[a]	q_{H1}	d(Si···C1)	d(C···H1)	∠(Si)
$Me_3Si-H-SiMe_3$	1.816	0.330	−0.340			348.1
C_6H_6_TMS[b]	1.922	0.275	0.315	2.1962	1.0952	342.4
1Me_C_6H_5_4TMS[c]	1.910	0.297	0.318	2.1464	1.0955	341.0
1,2Me_2_C_6H_4_4TMS[c]	1.912	0.301	0.318	2.1421	1.0956	340.5
1,3Me_2_C_6H_4_4TMS[c]	1.907	0.309	0.315	2.1323	1.0964	338.5
1,4Me_2_C_6H_4_2TMS[c]	1.915	0.296	0.313	2.1587	1.0962	338.7
1,2,3Me_3_C_6H_3_4TMS[c]	1.909	0.311	0.314	2.1296	1.0961	338.0
1,2,4Me_3_C_6H_3_5TMS[c]	1.908	0.313	0.315	2.1253	1.0964	337.7
1,3,5Me_3_C_6H_3_2TMS[c]	1.902	0.320	0.309	2.1258	1.0970	335.0
1,2,3,4Me_4_C_6H_2_5TMS[c]	1.909	0.316	0.314	2.1204	1.0964	337.4
1,2,3,5Me_4_C_6H_2_4TMS[c]	1.904	0.322	0.309	2.1230	1.0970	334.5
1,2,4,5Me_4_C_6H_2_3TMS[c]	1.910	0.312	0.308	2.1424	1.0970	334.8
1,2,3,4,5Me_5_C_6H_1_6TMS[c]	1.905	0.327	0.308	2.1130	1.0971	334.0
1Me_6_C_6_1TMS	1.923	0.318		2.1534		331.2
1Et_C_6H_5_4TMS[c]	1.910	0.299	0.318	2.1437	1.0955	340.7
1,3,5Et_3_C_6H_3_2TMS[c]	1.906	0.320	0.308	2.1222	1.0973	334.2
1-*n*-Pr_C_6H_5_4TMS[c]	1.909	0.300	0.318	2.1422	1.0955	340.7
1-*i*-Pr_C_6H_5_4TMS[c]	1.910	0.300	0.318	2.1419	1.0955	340.7
1,3,5-*i*-Pr_3_C_6H_3_2TMS[c]	1.903	0.328	0.309	2.1119	1.0982	333.2
1-*n*-Bu_C_6H_5_4TMS[c]	1.908	0.302	0.318	2.1381	1.0956	340.6
1-*t*-Bu_C_6H_5_4TMS[c]	1.909	0.301	0.318	2.1394	1.0955	340.4

[a] $Q_{CT} = 1 - \Sigma q_i(SiMe_3)$. [b] TMS = trimethylsilyl. [c] Only the lowest lying isomer is considered. [d] Notation: $x$$R_n$_$C_6H_n$_$y$TMS with x and y = numerals describing the positions in the arene.

Substitution of the methyl group by ethyl, *n*-propyl, isopropyl, or *n*-butyl groups only marginally affects the structural data (Table 2); e.g., the Si···C1 distances slightly decrease along H (2.1962 Å) < Me (2.1464 Å) < Et (2.1437 Å) < *n*-Pr (2.1422 Å) < *n*-Bu (2.1394 Å).

While the interaction of the silylium ion with benzene and hexamethyl benzene gives only one species, in the case of all other species of the type $Me_nC_6H_{6-n}$ ($n = 0-6$), in principle, at least two different isomers should be observed since silylation of the corresponding substituted arene might occur at the carbon arene atom attached to either a hydrogen atom or a methyl (alkyl) group. Additionally, silylation can also occur in the *ortho*, *meta*, or *para* position of the carbon ring atom bearing a methyl group, with the *para*-substituted isomer always being the lowest lying isomer. For example, for toluene four different isomers have been calculated (see the Supporting Information). The *para*-substituted isomer is energetically preferred over the *ortho* and *meta* compounds by $\Delta G_{298} = 2.88$ and 2.65 kcal mol^{-1}, respectively, in accord with the experimentally observed $[Me_3Si\cdot$*p*-toluene$]^+$ species (Figure 2). The energy difference between both *ortho* and *meta* isomers is rather small (0.23 kcal mol^{-1}). The isomer with the silylium ion in the 1-position (methyl and Me_3Si attached at C1, isomer 4) is always the highest lying isomer (7.64 kcal mol^{-1}). The energetically preferred species always show the smallest Si···C1 distances (*para*, 2.146 Å; *meta*, 2.173 Å; *ortho*, 2.178 Å; isomer 4, 2.283 Å).

A similar picture is found for all other $R_nC_6H_{6-n}$ ($n = 0-6$) (R = alkyl) species, which we do not want to discuss here in detail. In Tables 3 and 4 only data of the lowest lying isomers are presented (a complete set of data is listed in the Supporting Information). The isomers with the Me_3Si group attached to a ring carbon atom bearing a methyl group is unfavored by 4−7 kcal mol^{-1} with respect to the *para*-substituted species, while the *para*-substituted species is favored by about 2 kcal mol^{-1} over the *meta*/*ortho* species.

2.4.2. Energies and Charge Distribution. $[Me_3Si\cdot arene]^+$ ions can be considered as solvent complexes between arene and $[Me_3Si]^+$. In these complexes the Me_3Si fragment has almost completely lost its silylium character (strong deviation from planarity, Tables 1−3), since a stable bonded tetracoordinated Si center is formed. In this context and in analogy to the proton affinity, a trimethylsilylium affinity (TMSA) can be defined as the enthalpy change associated with the dissociation of the conjugated acid:[25a,46]

$$[Me_3Si\cdot B]^+_{(g)} \rightarrow B_{(g)} + [Me_3Si]^+_{(g)} \quad (\Delta H_{298}) \qquad (1)$$

TMSA values ($\Delta H_{(gas,298\ K)}$) describe the energetics of the desilylation reaction of a trimethylsilylium ion donor in the gas phase at 298 K, and small gas-phase TMSA values in comparison with that of unsubstituted benzene can be regarded a measure of stabilization in substituted benzenes. Furthermore, with the help of TMSA values, it is possible to decide if silylation transfer reactions are feasible, e.g., between R−X and $[Me_3Si\cdot arene]^+$ (X = H, halogen, any basic center). Table 4 summarizes TMSA and Gibbs free energies of all considered arene species (lowest lying isomer) at 298 K along with those of B (= Me_3Si-X; X = H, halogen, and pseudo-halogen) for comparison. The TMSA value of benzene amounts to 25.83 kcal mol^{-1}, which is, astonishingly, smaller than that of Me_3Si-H, 31.30 kcal mol^{-1} (cf. $TMSA_{halogen}$ between 31 and 35 kcal mol^{-1}). This means that $[Me_3Si\cdot benzene]^+$ is a stronger silylating agent than $[Me_3Si-H-SiMe_3]^+$ in the gas phase when solvent effects (liquid phase) or solid-state effects (solid phase) are impossible. However, it can be assumed

Table 4. TMSA Values (ΔH_{298}) Along with ΔE_0 and ΔG_{298} Values (kcal mol^{-1}) of Substituted [$Me_3Si\cdot$arene]$^+$ and [$Me_3Si-X-SiMe_3$]$^+$ Ions (X = H, Halogen, Pseudo-Halogen)

cation[a]	ΔE_0	ΔH_{298}	ΔG_{298}
TMS−H−TMS	34.53	31.30	23.23
TMS−F−TMS	38.02	34.79	26.79
TMS−Cl−TMS	34.43	31.05	21.60
TMS−Br−TMS	35.11	31.78	22.62
TMS−I−TMS	36.23	33.07	25.15
TMS−CN−TMS	58.20	54.44	45.65
TMS_2-N_3	47.80	44.23	32.90
TMS−NCO−TMS	42.16	39.34	27.82
TMS−NCS−TMS	44.49	41.14	31.49
TMS−NCSe−TMS	46.63	43.29	34.84
C_6H_6_TMS	29.37	25.83	15.63
1Me_C_6H_5_4TMS	33.78	30.92	19.31
1,2Me_2_C_6H_4_4TMS	35.94	32.48	22.33
1,3Me_2_C_6H_4_4TMS	36.80	33.21	21.96
1,4Me_2_C_6H_4_2TMS	34.93	31.25	19.56
1,2,3Me_3_C_6H_3_4TMS	37.09	33.37	18.72
1,2,4Me_3_C_6H_3_5TMS	38.79	35.21	24.13
1,3,5Me_3_C_6H_3_2TMS	39.01	35.27	21.02
1,2,3,4Me_4_C_6H_2_5TMS	40.64	37.07	25.98
1,2,3,5Me_4_C_6H_2_4TMS	40.58	36.87	24.45
1,2,4,5Me_4_C_6H_2_3TMS	38.35	34.75	23.91
1,2,3,4,5Me_5_C_6H_1_6TMS	42.29	38.59	27.13
1Me_6_C_6_1TMS	40.61	36.51	22.71
1Et_C_6H_5_4TMS	34.35	30.81	20.83
1,3,5Et_3_C_6H_3_2TMS	40.04	36.19	23.81
1-*n*-Pr_C_6H_5_4TMS	34.93	31.40	21.53
1-*i*-Pr_C_6H_5_4TMS	34.92	31.30	21.47
1,3,5-*i*-Pr_3_C_6H_3_2TMS	40.81	37.44	23.45
1-*n*-Bu_C_6H_5_4TMS	35.41	31.80	21.48
1-*t*-Bu_C_6H_5_4TMS	35.49	31.91	21.70

[a] Notation: xR_n_C_6H_n_yTMS with x and y = numerals describing the positions in the arene. TMS = trimethylsilyl, and TMSA = trimethylsilyl affinity.

that in solution as well in the solid state interactions with the environment (as discussed before) stabilize [$Me_3Si\cdot$benzene]$^+$ relative to [$Me_3Si-H-SiMe_3$]$^+$. Taking the TMSA value for benzene as a reference, all considered substituted benzene species possess larger TMSA values ranging between 30 and 39 kcal mol^{-1}. The small TMSA of benzene and also toluene (TMSA = 30.92 kcal mol^{-1}) may explain why fast degradation leading to the formation of a [$Me_3Si-F-SiMe_3$]$^+$ salt is observed (see section 2.1). Upon increasing substitution, the TMSA value increases by at least 5 kcal mol^{-1} (C_6H_6, 25.83 kcal mol^{-1}; $Me_1C_6H_5$, 30.92 kcal mol^{-1}; $Me_2C_6H_4$, 33.21 kcal mol^{-1}; $Me_3C_6H_3$, 35.27 kcal mol^{-1}; $Me_4C_6H_2$, 37.07 kcal mol^{-1}; $Me_5C_6H_1$, 38.59 kcal mol^{-1}). Due to steric reasons in Me_6C_6, the TMSA value (36.51 kcal mol^{-1}) decreases compared to that of $Me_5C_6H_1$. This trend nicely corresponds to the trend discussed for the Si···C1 distances. Only small changes (30.92−31.80 kcal mol^{-1}) are computed when the methyl group is substituted by ethyl, *n*-propyl, isopropyl, *n*-butyl or *tert*-butyl. Finally, it might be of interest to compare the TMSA values with proton affinities (PAs). The TMSA values of benzene and its derivatives are lower by about 161 kcal mol^{-1} than the corresponding proton affinities (cf. TMSA (kcal mol^{-1})/PA (kcal mol^{-1}): 25.8/183.3, benzene; 30.9/189.8, toluene; 33.2/195.9, *m*-xylol; 32.5/193.3, *o*-xylol; 31.3/192.0, *p*-xylol; 35.3/200.7, mesitylene).[47]

The Si···C1 bond in [$Me_3Si\cdot$arene]$^+$ ions might be regarded a donor−acceptor bond that can be characterized by the charge transfer from the arene into the Me_3Si^+ ion (Table 3), which becomes less positive. For the [$Me_3Si\cdot$benzene]$^+$ ion an overall charge transfer of 0.275*e* is found. The hydrogen atom attached to C1 suffers the largest loss of electron density upon complex formation (C_6H_6, q_{H1} = 0.237*e*; [$Me_3Si\cdot$benzene]$^+$, $q_{H1,cation}$ = 0.315*e*; cf. $q_{H2-6,cation}$ between 0.269*e* and 0.271*e*). A closer look into the charge transfer displays that the overall charge transfer can mainly be attributed to the arene hydrogen atoms (89.5%). With increasing degree of substitution, the charge transfer slightly increases (C_6H_6, 0.275*e*; $Me_1C_6H_5$, 0.297*e*; $Me_2C_6H_4$, 0.309*e*; $Me_3C_6H_3$, 0.320*e*; $Me_4C_6H_2$, 0.322*e*; $Me_5C_6H_1$, 0.327*e*). Substitution with a longer alkyl chain also only marginally increases the overall charge transfer ($Me_1C_6H_5$, 0.297*e*; $Et_1C_6H_5$, 0.299*e*; *n*-$Pr_1C_6H_5$, 0.300*e*; *n*-$Bu_1C_6H_5$, 0.302*e*).

It is interesting to mention that for the [$Me_3Si-H-SiMe_3$]$^+$ ion the charge transfer of 0.330*e* exclusively stems from the Me_3Si moiety of the Me_3Si-H fragment. Moreover, the bridging H atoms become even more negative upon complex formation (Me_3Si-H, q_H = −0.200*e*; [$Me_3Si-H-SiMe_3$]$^+$, $q_{H,cation}$ = −0.340*e*), which in turn means that the hydride character in [$Me_3Si-H-SiMe_3$]$^+$ is increased compared to that in Me_3Si-H. This also means that the Me_3Si moiety of the Me_3Si-H fragment decreases its charge by 0.47*e* (= 0.33*e* + 0.14*e* = $Q_{CT} + \Delta q_H$) upon complexation.

2.5. Conclusions. A simple synthetic route to solvent-coordinated [$Me_3Si\cdot$arene][$B(C_6F_5)_4$] salts (arene = benzene, toluene, ethylbenzene, *n*-propylbenzene, isopropylbenzene, *o*-xylene, *m*-xylene, *p*-xylene, 1,2,3-trimethylbenzene, 1,2,4-trimethylbenzene, 1,3,5-trimethylbenzene) starting from [$Me_3Si-H-SiMe_3$]-[$B(C_6F_5)_4$] has been described. This formal Lewis acid−Lewis base reaction allows preparation of large quantities in good yields. [$Me_3Si\cdot$arene][$B(C_6F_5)_4$] salts are air and moisture sensitive but stable under an argon atmosphere over a long period as solids but slowly decompose in solution even at ambient temperatures. They are thermally stable up to over 80 °C. Between 88 °C (benzene) and 118 °C (1,2,3-trimethylbenzene, hemimellitene), decomposition occurs, which is triggered by the formation of Me_3Si-F. Investigation of the degradation of [$Me_3Si\cdot$arene][$B(C_6F_5)_4$] revealed the formation of the fluoronium salt [$Me_3Si-F-SiMe_3$][$B(C_6F_5)_4$], $B(C_6F_5)_3$, and a reactive "C_6F_4" species which could be trapped by CS_2. Upon addition of CS_2, the formation of a formal S-heterocyclic carbene adduct, $C_6F_4CS_2-B(C_6F_5)_3$, was observed. The synthetic protocol described above does not work for *tert*-butylbenzene. Here the formation of [$Me_3Si-F-SiMe_3$][$B(C_6F_5)_4$] and 1,4-di-*tert*-butylbenzene was observed, which can be referred to as a Friedel−Crafts-type isomerization. Computations and X-ray structure elucidation reveal a tetracoordinated Si atom with a long Si···$C1_{arene}$ distance and an angle sum at Si considerably smaller than 360°. The Si···C1 coordination mode is always η^1 rather than η^2 or η^6. Due to very flat potential energy surfaces, the molecular structure parameters (e.g., d(Si−C1), $\Sigma\angle$(Si)) of the [$Me_3Si\cdot$arene]$^+$ ion strongly depend on the magnitude of interactions with the environment, such as anion−cation or cation−solvent interactions. If solvent molecules are in the proximity of the [$Me_3Si\cdot$arene]$^+$ ion, the solvent molecule is closely arranged to the cation and clearly directed toward the $H1_{cation}$ ring proton in η^6-type coordination mode with $H_{cation,arene}\cdots C_{solvent,arene}$ distances between 2.80 and 3.20 Å. This solvent−cation interaction is further supported by a significantly larger displacement of the $H1_{cation,arene}$ proton from the arene ring plane as indicated by the H1−C1−C2−C6 dihedral angle (−147° vs −155° for all other nonsolvate species). Furthermore, NPA partial charge calculations reveal that $H1_{cation,arene}$ always carries the largest positive charge within the ring (Table 3), about 0.32*e* (cf. 0.23*e*−0.27*e* for all other arene protons), and even the protons of the Me_3Si unit are less positive (0.27*e*−0.29*e*).

Since very flat potential energy surfaces are observed for the systems $[Me_3Si\cdot arene]^+$ with respect to C−Si−C and Si−C1−H1 angles and the donor−acceptor bond (Si···C1 distance), consistent structural trends are only obtained for isolated species in the gas phase when environmental effects are excluded. A systematic study of the influence of the arene substitution pattern in $[Me_3Si\cdot arene][B(C_6F_5)_4]$ (arene = $R_nC_6H_{6-n}$, R = H, Me, Et, Pr, and Bu; $n = 0-6$) shows the following general trends: (i) *para* substitution with respect to the alkyl group is always favored over *ortho* or *meta* isomers (by ca. 2 kcal mol^{-1}). (ii) With increasing degree of substitution, the shorter the Si···C1 distance (between 2.196 Å $[Me_3Si\cdot benzene]^+$ and 2.113 Å $[Me_3Si\cdot Me_5C_6H_1]$), the larger the overall charge transfer (between 0.275*e* $[Me_3Si\cdot benzene]^+$ and 0.327*e* $[Me_3Si\cdot Me_5C_6H_1]$) and the larger the calculated TMSA value (between 25.83 kcal mol^{-1} $[Me_3Si\cdot benzene]^+$ and 38.59 kcal mol^{-1} $[Me_3Si\cdot Me_5C_6H_1]$). The TMSA values can be regarded a measure of stabilization in substituted benzenes. Furthermore, with the help of a TMSA scale, it is possible to decide if silylation transfer reactions are feasible, e.g., between R−X and $[Me_3Si\cdot arene]^+$ (X = H, halogen, any basic center). From this scale, it can be concluded that in the gas phase the strongest Me_3Si^+ transfer reagent is $[Me_3Si\cdot benzene]^+$, even stronger than $[Me_3Si{-}H{-}SiMe_3]^+$ (TMSA = 31.30 kcal mol^{-1}).

3. EXPERIMENTAL DETAILS

3.1. General Information. All manipulations were carried out under oxygen- and moisture-free conditions under argon using standard Schlenk or drybox techniques.

Benzene (99.7%, Sigma-Aldrich), toluene (99.7%, Sigma-Aldrich), ethylbenzene (VEB Berlin, Berlin Adlershof), *n*-propylbenzene (98%, Aldrich), isopropylbenzene (97%, Ferak Chemikalien, Berlin), *tert*-butylbenzene (97%, Fluka), *m*-xylene (97%, Reachim), *p*-xylene (97%, VEB Teerdestilation and Chemische Fabrik, Erkner), *o*-xylene (97%, VEB Petrolchemisches Kombinat Schwedt, BT Erkner), 1,2,3-trimethylbenzene (95%, Fluka), 1,2,4-trimethylbenzene (techn., VEB Teerdestilation and Chemische Fabrik, Erkner), and 1,3,5-trimethylbenzene (98%, Merck) were dried over Na/benzophenone and freshly distilled prior to use. *n*-Heptane was freshly distilled prior to use. Bis(trimethylsilyl)hydronium tetrakis(pentafluorophenyl)borate ($[Me_3Si{-}H{-}SiMe_3][B(C_6F_5)_4]$, structure C) was prepared as previously reported.[5b,24b]

3.1.1. NMR Spectroscopy. $^{13}C\{^1H\}$, ^{13}C DEPT (distortionless enhancement by polarization transfer), and ^1H NMR spectra were obtained on a Bruker AVANCE 300 spectrometer and were referenced internally to the deuterated solvent (^{13}C, $CDCl_3$, $\delta_{reference}$ = 77 ppm) or to protic impurities in the deuterated solvent (^1H, $CHCl_3$, $\delta_{reference}$ = 7.26 ppm). $CDCl_3$ was dried over P_4O_{10} and freshly distilled prior to use.

3.1.2. IR Spectroscopy. A Nicolet 6700 FT-IR spectrometer with a Smart Endurance attenuated total reflectance (ATR) device was used.

3.1.3. Raman Spectroscopy. A Bruker VERTEX 70 FT-IR spectrometer with an RAM II FT-Raman module equipped with a Nd:YAG laser (1064 nm) was used.

3.1.4. CHN Analyses. A C/H/N/S-Mikronalysator TruSpec-932 from Leco was used.

3.1.5. Differential Scanning Calorimetry (DSC). A DSC 823e from Mettler-Toledo (heating rate 5 °C/min) was used.

3.2. General Procedure for the Synthesis of Trimethylsilicenium−Arene Salts $[Me_3Si\cdot arene][B(C_6F_5)_4]$ (Arene = Benzene, Toluene, Ethylbenzene, *n*-Propylbenzene, Isopropylbenzene, *o*-Xylene, *m*-Xylene, *p*-Xylene, 1,2,3-Trimethylbenzene, 1,2,4-Trimethylbenzene, and 1,3,5-Trimethylbenzene). To neat bis(trimethylsilyl)hydronium tetrakis(pentafluorophenyl)borate ($[Me_3Si{-}H{-}SiMe_3][B(C_6F_5)_4]$, structure C) (0.413 g, 0.5 mmol) was added a minimum of the corresponding arene (3−5 mL) at ambient temperature with stirring, followed by gentle heating to 80 °C until a clear colorless solution and an oiled-out layer was obtained. Slow cooling to ambient temperature over a period of 1 h resulted in the deposition of colorless crystals. Removal of excess arene by decantation and drying in vacuo gave the corresponding trimethylsilicenium−arene tetrakis(pentafluorophenyl)borate ($[Me_3Si\cdot arene][B(C_6F_5)_4]$ (arene = benzene, toluene, ethylbenzene, *n*-propylbenzene, isopropylbenzene, *o*-xylene, *m*-xylene, *p*-xylene, 1,2,3-trimethylbenzene, 1,2,4-trimethylbenzene, 1,3,5-trimethylbenzene)) as a colorless solid in good yield (70−90%).

3.2.1. $[Me_3Si\cdot C_6H_6][B(C_6F_5)_4]$ (Benzene). Mp: 88 °C (dec. Anal. Calcd for $[Me_3Si\cdot C_6H_6][B(C_6F_5)_4]$ (Found): C, 47.73 (45.98); H, 1.82 (1.45). IR (ATR, 16 scans, cm^{-1}): 3113 (w), 3092 (w), 3034 (w), 2996 (w), 2914 (w), 1643 (m), 1600 (w), 1588 (w), 1556 (w), 1513 (s), 1455 (s), 1412 (m), 1383 (m), 1372 (m), 1342 (m), 1321 (m), 1271 (m), 1180 (w), 1164 (w), 1082 (s), 1034 (w), 1022 (w), 972 (s), 912 (w), 869 (m), 856 (w), 813 (m), 770 (m), 755 (m), 737 (m), 728 (w), 698 (m), 683 (m), 662 (s), 623 (m), 611 (w), 603 (w), 573 (m).

3.2.2. $[Me_3Si\cdot C_7H_8][B(C_6F_5)_4]$ (Toluene). Mp: 108 °C dec. Anal. Calcd for $[Me_3Si\cdot C_7H_8][B(C_6F_5)_4]$ (Found): C, 48.36 (48.01); H, 2.03 (1.76). IR (ATR, 16 scans, cm^{-1}): 3092 (w), 3014 (w), 2979 (w), 2914 (w), 2042 (w), 2016 (w), 1987 (w), 1644 (m), 1598 (w), 1556 (w), 1513 (s), 1456 (s), 1413 (m), 1380 (m), 1321 (m), 1271 (m), 1261 (m), 1216 (w), 1190 (w), 1179 (w), 1145 (w), 1082 (s), 1022 (w), 998 (m), 972 (s), 918 (w), 865 (m), 820 (s), 799 (s), 774 (s), 755 (s), 735 (w), 727 (w), 694 (m), 683 (m), 659 (s), 624 (m), 610 (w), 603 (w), 573 (m).

3.2.3. $[Me_3Si\cdot C_8H_{10}][B(C_6F_5)_4]\cdot C_8H_{10}$ (Ethylbenzene). Mp: 112 °C dec. Anal. Calcd for $[Me_3Si\cdot C_8H_{10}][B(C_6F_5)_4]\cdot C_8H_{10}$ (Found): C, 53.54 (53.35); H, 3.03 (3.13). IR (ATR, 16 scans, cm^{-1}): 3084 (w), 3063 (w), 3028 (w), 2969 (w), 2936 (w), 2913 (w), 2877 (w), 1643 (m), 1615 (w), 1597 (w), 1562 (w), 1556 (w), 1512 (s), 1456 (s), 1412 (m), 1382 (m), 1374 (m), 1341 (w), 1327 (w), 1270 (m), 1263 (m), 1186 (w), 1082 (s), 1037 (w), 1031 (w), 973 (s), 923 (w), 907 (w), 863 (m), 809 (m), 773 (s), 770 (s), 755 (s), 726 (m), 700 (m), 683 (m), 660 (s), 623 (m), 610 (m), 603 (m), 573 (m), 558 (m).

3.2.4. $[Me_3Si\cdot C_9H_{12}][B(C_6F_5)_4]$ (n-Propylbenzene). Mp: 87 °C dec. Anal. Calcd for $[Me_3Si\cdot C_9H_{12}][B(C_6F_5)_4]$ (Found): C, 49.56 (47.46); H, 2.43 (2.00). IR (ATR, 16 scans, cm^{-1}): 3089 (w), 3009 (w), 2973 (w), 2939 (w), 2879 (w), 1644 (m), 1644 (w), 1610 (w), 1595 (w), 1563 (w), 1556 (w), 1513 (s), 1456 (s), 1412 (m), 1381 (m), 1375 (m), 1322 (m), 1271 (m), 1188 (w), 1180 (w), 1162 (w), 1144 (w), 1082 (s), 1028 (w), 1011 (w), 972 (s), 921 (m), 909 (w), 861 (m), 811 (m), 774 (s), 769 (s), 755 (s), 726 (m), 711 (w), 683 (m), 661 (s), 623 (m), 611 (m), 603 (m), 573 (m).

3.2.5. $[Me_3Si\cdot C_9H_{12}][B(C_6F_5)_4]$ (Isopropylbenzene, Cymene). Mp: 95 °C dec. Anal. Calcd for $[Me_3Si\cdot C_9H_{12}][B(C_6F_5)_4]$ (Found): C, 49.56 (49.12); H, 2.43 (2.13). IR (ATR, 16 scans, cm^{-1}): 3099 (w), 3014 (w), 3013 (w), 2974 (w), 2936 (w), 2914 (w), 2875 (w), 1644 (m), 1611 (w), 1595 (w), 1557 (w), 1557 (w), 1512 (s), 1457 (s), 1413 (m), 1381 (m), 1375 (m), 1367 (m), 1325 (w), 1271 (m), 1261 (m), 1192 (w), 1164 (w), 1080 (s), 1048 (w), 1029 (w), 998 (m), 974 (s), 922 (m), 908 (w), 865 (m), 853 (m), 834 (w), 808 (s), 774 (s), 768 (s), 756 (s), 725 (m), 702 (w), 683 (m), 660 (s), 622 (m), 611 (m), 603 (m), 573 (m), 563 (w), 538 (m).

3.2.6. $[Me_3Si\cdot C_8H_{10}][B(C_6F_5)_4]$ (1,2-Dimethylbenzene, o-Xylene). Mp: 91 °C (106 °C dec). Anal. Calcd for $[Me_3Si\cdot C_8H_{10}][B(C_6F_5)_4]$ (Found): C, 48.97 (48.40); H, 2.23 (1.80). IR (ATR, 16 scans, cm^{-1}): 3013 (w), 2975 (w), 2915 (w), 2874 (w), 1644 (m), 1595 (w), 1556 (w), 1512 (s), 1455 (s), 1412 (m), 1381 (m), 1374 (m), 1321 (w), 1270 (m), 1262 (m), 1188 (w), 1179 (w), 1161 (w), 1081 (s), 1035 (w), 972 (s), 938 (m), 895 (w), 858 (m), 823 (m), 801 (m), 773 (s), 768 (s), 755 (s), 727 (m), 696 (m), 683 (s), 661 (s), 622 (m), 610 (m), 603 (m), 573 (w).

3.2.7. $[Me_3Si\cdot C_8H_{10}][B(C_6F_5)_4]\cdot C_8H_{10}$ (1,3-Dimethylbenzene, m-Xylene). Mp: 104 °C dec. Anal. Calcd for $[Me_3Si\cdot C_8H_{10}][B(C_6F_5)_4]$ (Found): C, 48.97 (50.64); H, 2.23 (2.59). IR (ATR, 16 scans, cm^{-1}): 3013 (w), 2950 (w), 2918 (w), 2864 (w), 2734 (w), 1644 (m), 1620 (w), 1601 (w), 1558 (w), 1512 (s), 1455 (s), 1412 (m), 1374 (m), 1341 (w), 1325 (w), 1300 (w), 1270 (m), 1205 (w), 1176 (w), 1158 (w), 1144 (w), 1082 (s), 1031 (w), 998 (m), 972 (s), 924 (m), 907 (m), 862 (m), 818 (m), 808 (m), 773 (s), 756 (s), 727 (m), 715 (w), 692 (m), 683 (s), 660 (s), 624 (m), 610 (m), 603 (m), 574 (m), 543 (w), 530 (w).

3.2.8. $[Me_3Si\cdot C_8H_{10}][B(C_6F_5)_4]\cdot C_8H_{10}$ (1,4-Dimethylbenzene, p-Xylene). Mp: 95 °C dec. Anal. Calcd for $[Me_3Si\cdot C_8H_{10}][B(C_6F_5)_4]$ (Found): C, 48.97 (48.75); H, 2.23 (2.29). IR (ATR, 16 scans, cm^{-1}): 2995 (w), 2974 (w), 2961 (w), 2923 (w), 2872 (w), 1643 (m), 1622 (w), 1613 (w), 1600 (w), 1556 (w), 1512 (s), 1456 (s), 1412 (m), 1380 (m), 1375 (m), 1323 (w), 1270 (m), 1211 (w), 1183 (w), 1145 (w), 1081 (s), 1038 (w), 1030 (w), 995 (m), 974 (s), 924 (m), 904 (m), 861 (m), 821 (m), 802 (s), 773 (s), 755 (s), 725 (m), 703 (w), 682 (s), 659 (s), 622 (m), 610 (m), 602 (m), 573 (m), 553 (w), 544 (w).

3.2.9. $[Me_3Si\cdot C_9H_{12}][B(C_6F_5)_4]\cdot C_9H_{12}$ (1,2,3-Trimethylbenzene, Hemimellitene). Mp: 118 °C dec. Anal. Calcd for $[Me_3Si\cdot C_9H_{12}][B(C_6F_5)_4]\cdot C_9H_{12}$ (Found): C, 54.45 (54.25); H, 3.35 (2.61). IR (ATR, 16 scans, cm^{-1}): 3066 (w), 3041 (w), 3013 (w), 2944 (w), 2916 (w), 2871 (w), 2732 (w), 1643 (m), 1606 (w), 1586 (w), 1512 (s), 1456 (s), 1412 (m), 1375 (m), 1328 (w), 1270 (s), 1176 (w), 1082 (s), 1033 (w), 973 (s), 926 (m), 907 (w), 857 (m), 816 (m), 802 (m), 773 (s), 756 (s), 726 (m), 708 (m), 683 (m), 659 (s), 624 (m), 610 (m), 602 (m), 573 (m), 538 (m).

3.2.10. $[Me_3Si\cdot C_9H_{12}][B(C_6F_5)_4]\cdot C_9H_{12}$ (1,2,4-Trimethylbenzene, Pseudo-Cymene). Mp: 115 °C dec. Anal. Calcd for $[Me_3Si\cdot C_9H_{12}][B(C_6F_5)_4]\cdot C_9H_{12}$ (Found): C, 54.45 (53.19); H, 3.35 (2.61). IR (ATR, 16 scans, cm^{-1}): 2962 (w), 2943 (w), 2925 (w), 2873 (w), 2735 (w), 1643 (m), 1620 (w), 1604 (w), 1556 (w), 1512 (s), 1457 (s), 1413 (m), 1375 (m), 1320 (w), 1271 (s), 1259 (m), 1154 (w), 1082 (s), 1030 (w), 974 (s), 924 (w), 908 (w), 872 (m), 853 (m), 815 (s), 773 (s), 756 (s), 726 (m), 695 (w), 683 (s), 660 (m), 622 (m), 610 (m), 602 (m), 573 (m), 540 (m).

3.2.11. $[Me_3Si\cdot C_9H_{12}][B(C_6F_5)_4]\cdot C_9H_{12}$ (1,3,5-Trimethylbenzene, Mesitylene). Mp: 89 °C (116 °C dec). Anal. Calcd for $[Me_3Si\cdot C_9H_{12}][B(C_6F_5)_4]\cdot C_9H_{12}$ (Found): C, 53.34 (53.47); H, 3.14 (2.61). IR (ATR, 16 scans, cm^{-1}): 3011 (w), 2953 (w), 2916 (w), 2862 (w), 1643 (m), 1622 (w), 1600 (m), 1556 (w), 1512 (s), 1457 (s), 1412 (m), 1381 (m), 1374 (m), 1338 (w), 1293 (w), 1272 (m), 1259 (m), 1161 (w), 1153 (w), 1082 (s), 1032 (w), 999 (m), 975 (s), 933 (m), 917 (m), 853 (m), 841 (m), 815 (s), 773 (s), 755 (s), 726 (m), 683 (s), 660 (s), 631 (m), 611 (m), 603 (m), 573 (m), 537 (m).

■ ASSOCIATED CONTENT

Ⓢ **Supporting Information.** Experimental and computational details, crystallographic information (CIF), further experimental and theoretical data of all considered species, and complete ref 43. This material is available free of charge via the Internet at http://pubs.acs.org.

■ AUTHOR INFORMATION

Corresponding Author

axel.schulz@uni-rostock.de; alexander.villinger@uni-rostock.de

■ ACKNOWLEDGMENT

We are indebted to Nick Hartmann and Dr. Jeanette Stelter (University of Rostock, Entsorgungshof) for the kind gift of chemicals. Martin Ruhmann (University of Rostock) is acknowledged for the measurement of the Raman spectra. Financial support by the Deutscher Akademischer Austausch Dienst (DAAD; German Academic Exchange Service) (scholarship for M.F.I.) is gratefully acknowledged. Financial support by the Deutsche Forschungsgemeinschaft (DFG; German Research Foundation) (Grant 1170/6-1) is gratefully acknowledged.

■ REFERENCES

(1) Lambert, J. B; Kania, L.; Zhang, S. *Chem. Rev.* **1995**, *95*, 1191–1201.

(2) In contrast, siliconium ions are positively charged species in which silicon has higher than four-coordination. Some authors prefer to restrict the term silylium ion to the fully tricoordinate form. See also: http://old.iupac.org/publications/books/rbook/Red_Book_2005.pdf.

(3) (a) Maerker, C.; Kapp, J.; Schleyer, P. v. R. In *Organosilicon Chemistry II*; Auner, N., Weis, J., Eds.; VCH: Weinheim, Germany, 1996; pp 329−358. (b) Reed, C. A. *Acc. Chem. Res.* **1998**, *31*, 325. (c) Lickiss, P. In *The Chemistry of Organic Silicon Compounds*, 2nd ed.; Rappoport, Z., Apeloig, Y., Eds.; Wiley: Chichester, U.K., 1998; Chapter 11. (d) Lambert, J. B.; Zhao, Y.; Zhang, S. M. *J. Phys. Org. Chem.* **2001**, *14*, 370.

(4) Kim, K.-C.; Reed, C. A.; Elliott, D. W.; Mueller, L. J.; Tham, F.; Lin, L.; Lambert, J. B. *Science* **2002**, *297*, 825.

(5) (a) Lambert, J. B.; Zhang, S.; Stern, C. L.; Huffman, J. C. *Science* **1993**, *260*, 1917–1918. (b) Lambert, J. B.; Zhang, S.; Ciro, S. M. *Organometallics* **1994**, *13*, 2430–2443.

(6) Xie, Z.; Liston, D. J.; Jelinek, T.; Mitro, V.; Bau, R.; Reed, C. A. *J. Chem. Soc., Chem. Commun.* **1993**, 384–386.

(7) Duttwyler, S.; Do, Q.; Linden, A.; Baldridge, K. K.; Siegel, J. S. *Angew. Chem.* **2008**, *120*, 1743–1746. *Angew. Chem., Int. Ed.* **2008**, *47*, 1719–1722.

(8) Müller, T.; Bauch, C.; Ostermeier, M.; Bolte, M.; Auner, N. *J. Am. Chem. Soc.* **2003**, *125*, 2158–2168.

(9) Hara, K.; Akiyama, R.; Sawamura, M. *Org. Lett.* **2005**, *7*, 5621.

(10) For Lewis base activation of silicon Lewis acids, see: Denmark, S. E.; Chung, W. *J. Org. Chem.* **2008**, *73*, 4582.

(11) (a) Scott, V. J.; Elenligiletin, R.; Ozerov, O. V. *J. Am. Chem. Soc.* **2005**, *127*, 2852–2853. (b) Douvris, C.; Ozerov, O. V. *Science* **2008**, *321*, 1188–1190.

(12) Panisch, R.; Bolte, M.; Müller, T. *J. Am. Chem. Soc.* **2006**, *128*, 9676–9682.

(13) Klare, H. F. T.; Bergander, K.; Oestreich, M. *Angew. Chem.* **2009**, *121*, 9241–9243. *Angew. Chem., Int. Ed.* **2009**, *48*, 9077–9079.

(14) Meier, G.; Braun, T. *Angew. Chem.* **2009**, *121*, 1575–1577. *Angew. Chem., Int. Ed.* **2009**, *48*, 1546–1548.

(15) Zhang, Y.; Huynh, K.; Manners, I.; Reed, C. A. *Chem. Commun.* **2008**, 494–496.

(16) (a) Lambert, J. B.; Zhao, Y. *Angew. Chem.* **1997**, *109*, 389–391. *Angew. Chem., Int. Ed. Engl.* **1997**, *36*, 400–401. (b) Lambert, J. B.; Zhao, Y.; Wu, H.; Tse, W. C.; Kuhlmann, B. *J. Am. Chem. Soc.* **1999**, *121*, 5001–5008.

(17) (a) Reed, C. A.; Xie, Z.; Bau, R.; Benesi, A. *Science* **1993**, *262*, 402–404. (b) Xie, Z.; Manning, J.; Reed, R. W.; Mathur, R.; Boyd, P. D. W.; Benesi, A.; Reed, C. A. *J. Am. Chem. Soc.* **1996**, *118*, 2922–2928.

(18) (a) Krossing, I.; Raabe, I. *Angew. Chem.* **2004**, *116*, 2116–2142. *Angew. Chem., Int. Ed.* **2004**, *43*, 2066–2090. (b) Strauss, S. H. *Chem. Rev.* **1993**, *93*, 927–942.

(19) (a) Pauling, L. *Science* **1994**, *263*, 983. (b) Reed, C. A.; Xie, Z. *Science* **1994**, *263*, 984. (c) Lambert, J. B.; Zhang, S. *Science* **1994**, *263*, 985. (d) Lambert, J. B.; Olah, G. A.; Rasul, G.; Li, X.; Buchholz, H. A.; Sandford, G.; Prakash, G. K. S. *Science* **1994**, *263*, 983.

(20) Schleyer, P.v.R.; Buzek, P.; Müller, T.; Apeloig, Y.; Siehl, H.-U. *Angew. Chem.* **1993**, *105*, 1558–1561. *Angew. Chem., Int. Ed. Engl.* **1993**, *32*, 1471–1473.

(21) Müller, T; Zhao, Y.; Lambert, J. B. *Organometallics* **1998**, *17*, 278–280.

(22) Olsson, L.; Ottosson, C.-H.; Cremer, D. *J. Am. Chem. Soc.* **1995**, *117*, 7460–7479.

(23) Arshadi, M.; Johnels, D.; Edlund, U.; Ottosson, C.-H.; Cremer, D. *J. Am. Chem. Soc.* **1996**, *118*, 5120–5131.

(24) (a) Schulz, A.; Villinger, A. *Chem.—Eur. J.* **2010**, *16*, 7276–7281. (b) Lehmann, M.; Schulz, A.; Villinger, A. *Angew. Chem.* **2009**, *121*, 7580–7583. *Angew. Chem., Int. Ed.* **2009**, *48*, 7444–7447.

(25) For halogen−Si coordination in silylium ions, see: (a) Küppers, T.; Bernhardt, E.; Eujen, R.; Willner, H.; Lehmann, C. W. *Angew. Chem., Int. Ed.* **2007**, *46*, 6346. (b) Hoffmann, S. P.; Kato, T.; Tham, F. S.; Reed, C. A. *Chem. Commun.* **2006**, 767. (c) Romanato, P.; Duttwyler, S.; Linden, A.; Baldridge, K. K.; Siegel, J. S. *J. Am. Chem. Soc.* **2010**, *132*, 7828–7829. (d) Sekiguchi, A.; Murakami, Y.; Fukaya, N.; Kabe, Y. *Chem. Lett.* **2004**, *33*, 520.

(26) Lambert, J. B.; Zhang, S. *J. Chem. Soc., Chem. Commun.* **1993**, 383–384.

(27) Reed, C. A.; Nava, M. *Organometallics* **2011**, *30*, 4798–4800.

(28) Lorcy, D.; Bellec, N.; Fourmigue, M.; Avarvari, N. *Coord. Chem. Rev.* **2009**, *253*, 1398–1438.

(29) All published attempted syntheses to prepare 1,3-dithiol-2-ylides (even with CS_2) led to the dimerization product tetrathiafulvalene. See for example: (a) Krebs, A.; Kimling, H. *Angew. Chem.* **1971**, *83*, 540–541. (b) Arduengo, A. J.; Goerlich, J. R.; Marshall, W. J. *Liebigs Ann./Recl.* **1997**, 365–374. (c) Fabian, J. *J. Org. Chem.* **2000**, *65*, 8940–8947.

(30) Ung, G.; Mendoza-Espinosa, D.; Bouffard, J.; Bertrand, G. *Angew. Chem., Int. Ed.* **2011**, *50*, 4215–4218.

(31) For reviews see: (a) *Friedel-Crafts and Related Reactions*; Olah, G. A., Ed.; Wiley: New York, 1963−1964; Vols. I−IV. (b) Olah, G. A. *Friedel-Crafts Chemistry*; Wiley-Interscience: New York, 1973.

(32) (a) Bowlus, H.; Nieuwland, J. *J. Am. Chem. Soc.* **1931**, *53*, 3835. (b) Meerwein, H.; Pannwitz, W. *J. Prakt. Chem.* **1934**, *141*, 123. (c) Booth, H. S.; Martin, D. R. *Boron Trifuoride and Its Derivatives*; Wiley: New York, 1949. (d) Topchiev, A. V.; Zavgorodnii, S. V.; Paushkin, Y. M. *Boron Trifluoride and Its Compounds as Catalysts in Organic Chemistry*, English edition; Pergamon: New York, 1959.

(33) Olah, G. A.; Prakash, G. K. S.; Sommer, J. *Superacids*; Wiley-Interscience: New York, 1985.

(34) (a) Olah, G. A.; Farooq, O.; Farnia, S. F. M.; Olah, J. A. *J. Am. Chem. Soc.* **1988**, *110*, 2560.

(35) (a) Lühmann, N.; Panisch, R.; Müller, T. *Appl. Organomet. Chem.* **2010**, *24*, 533–537. (b) Allemann, O.; Duttwyler, S.; Romanato, P.; Baldridge, K. K.; Siegel, J. S. *Science* **2011**, *332*, 574–577.

(36) Wiberg, H. *Lehrbuch der Anorganischen Chemie*, 102 Aufl.; Walter de Gruyter: Berlin, 2007; Anhang IV.

(37) Müller, T. *Adv. Organomet. Chem.* **2005**, *53*, 155.

(38) Xie, Z.; Bau, R.; Benesi, A.; Reed, C. A. *Organometallics* **1995**, *14*, 3933.

(39) Pyykkö, P; Atsumi, M. *Chem.—Eur. J* **2009**, *15*, 12770–12779.

(40) Phillips, A. D.; Power, P. P *Acta Crystallogr.* **2005**, *C61*, o291–o293.

(41) Holschumacher, D.; Bannenberg, T.; Hrib, C. G.; Jones, P. G.; Tamm, M. *Angew. Chem.* **2008**, *120*, 7538–7542. *Angew. Chem., Int. Ed.* **2008**, *47*, 7428–7432.

(42) Bernsdorf, A.; Brand, H.; Hellmann, R.; Köckerling, M.; Schulz, A.; Villinger, A.; Voss, K. *J. Am. Chem. Soc.* **2009**, *131*, 8958–8970.

(43) Frisch, M. J.; et al. *Gaussian 03*, revision E.01; Gaussian, Inc.: Wallingford, CT, 2004.

(44) (a) Dunning, T. H. *J. Chem. Phys.* **1989**, *90*, 1007. (b) Woon, D. E.; Dunning, T. H. *J. Chem. Phys.* **1993**, *98*, 1358. (c) Peterson, K. A.; Dunning, T. H. *J. Chem. Phys.* **2002**, *117*, 10548.

(45) (a) Glendening, E. D; Reed, A. E.; Carpenter, J. E.; Weinhold, F. NBO version 3.1. (b) Carpenter, J. E.; Weinhold, F. *J. Mol. Struct.: THEOCHEM* **1988**, *169*, 41. (c) Weinhold, F.; Carpenter, J. E. *The Structure of Small Molecules and Ions*; Plenum Press: New York, 1988; p 227. (d) Weinhold, F.; Landis, C. *Valency and Bonding. A Natural Bond Orbital Donor-Acceptor Perspective*; Cambridge University Press: Cambridge, U.K., 2005; see also references therein.

(46) (a) Olah, G. A. *Halonium Ions*; Wiley-Interscience: New York, 1975. (b) Olah, G. A.; Prakash, G. K. S.; Sommer, J. *Superacids*; John Wiley & Sons: New York, 1985. (c) Swart, M.; Rösler, E.; Bickelhaupt, M. *J. Comput. Chem.* **2006**, 1485–1492.

(47) Lias, S. G.; Liebman, J. F.; Levin, R. D. *J. Phys. Chem. Ref. Data* **1984**, *13*, 695–808.